



King Saud University  
Arabian Journal of Chemistry

www.ksu.edu.sa  
www.sciencedirect.com



## REVIEW

# Nontoxic corrosion inhibitors for N80 steel in hydrochloric acid



M. Yadav \*, Debasis Behera, Usha Sharma

Department of Applied Chemistry, ISM, Dhanbad 826004, India

Received 11 November 2011; accepted 17 March 2012

Available online 24 March 2012

## KEYWORDS

N80 steel;  
Imidazolines;  
Corrosion inhibitors;  
15% HCl;  
FTIR analysis

**Abstract** The purpose of this paper is to evaluate the protective ability of 1-(2-aminoethyl)-2-oleylimidazole (AEOI) and 1-(2-oleylamidoethyl)-2-oleylimidazole (OAEIO) as corrosion inhibitors for N80 steel in 15% hydrochloric acid, which may find application as eco-friendly corrosion inhibitors in acidizing processes in petroleum industry. Different concentrations of synthesized inhibitors AEOI and OAEIO were added to the test solution (15% HCl) and the corrosion inhibition of N80 steel in hydrochloric acid medium containing inhibitors was tested by weight loss, potentiodynamic polarization and AC impedance measurements. Influence of temperature (298–323 K) on the inhibition behavior was studied. Surface studies were performed by using FTIR spectra and SEM. Both the inhibitors, AEOI and OAEIO at 150 ppm concentration show maximum efficiency 90.26% and 96.23%, respectively at 298 K in 15% HCl solution. Both the inhibitors act as mixed corrosion inhibitors. The adsorption of the corrosion inhibitors at the surface of N80 steel is the root cause of corrosion inhibition.

© 2012 Production and hosting by Elsevier B.V. on behalf of King Saud University. This is an open access article under the CC BY-NC-ND license (<http://creativecommons.org/licenses/by-nc-nd/3.0/>).

## Contents

1. Introduction . . . . .	S1488
2. Experimental. . . . .	S1488
2.1. Synthesis of inhibitors . . . . .	S1489

\* Corresponding author. Tel.: +91 0326 2235428.

E-mail address: [yadav\\_drmahendra@yahoo.co.in](mailto:yadav_drmahendra@yahoo.co.in) (M. Yadav).

Peer review under responsibility of King Saud University.



3. Results and discussion . . . . .	S1490
3.1. Weight loss tests . . . . .	S1490
3.2. Electrochemical polarization studies . . . . .	S1491
3.3. Electrochemical impedance spectroscopy (EIS) . . . . .	S1491
3.4. Effect of temperature and thermodynamic parameters of inhibitor adsorption . . . . .	S1491
3.5. Adsorption isotherms . . . . .	S1492
3.6. SEM study . . . . .	S1494
3.7. FTIR spectroscopic analysis of corrosion product . . . . .	S1494
4. Discussion . . . . .	S1494
5. Conclusions . . . . .	S1494
References . . . . .	S1495

## 1. Introduction

The N80 carbon steel has been generally used as the main construction material for down hole tubular, flow lines and transmission pipelines in petroleum industry. Acidization of a petroleum oil well is one of the important stimulation techniques for enhancing oil production. It is commonly brought about by forcing a solution of 15–28% hydrochloric acid into the well to remove plugging in the bore well and stimulate production in petroleum industry. To reduce the aggressive attack of the acid on tubing and casing materials (N80 steel), inhibitors are added to the acid solution during the acidifying process (Allen and Roberts, 1982). In the previous work various organic inhibitors have been tested for the corrosion inhibition of N80 steel in hydrochloric medium (Vishwanatham and Sinha, 2009; Emranuzaman et al., 2004; Quraishi et al., 2002; Neemla et al., 1989). Corrosion protection of N80 steel in HCl by condensation products of aniline and phenol, (Vishwanatham and Sinha, 2009) was studied. Corrosion inhibition of N80 steel in hot hydrochloric acid medium by disalicylidene acetone, dicinnamylidene acetone and divanilidene acetone was reported (Quraishi et al., 2002). Despite the vast number of corrosion inhibition investigations, there remains relatively few works directed toward the study of non-toxic organic compounds as corrosion inhibitors for steel in hydrochloric acid (Yadav and Sharma, 2011; Khaled, 2008; Hluchan et al., 1998; Ashassi-Sorkhabi et al., 2004; Ghareba and Omanoic, 2010). The effective acidizing inhibitors that are usually found in commercial formulations, suffer from drawbacks, they are effective only at high concentrations and they are harmful to the environment due to their toxicity, so it is important to search for new non-toxic and effective organic corrosion inhibitors for N80 steel – 15% hydrochloric acid system.

Thus, it was considered interesting to prepare nontoxic imidazole compounds like 1-(2-aminoethyl)-2-oleylimidazole (AEOI) and 1-(2-oleylamidoethyl)-2-oleylimidazole (OAE-OI) and to assess their inhibitive properties for oil-well tubular steel (N80) in 15% hydrochloric acid.

## 2. Experimental

Rectangular steel coupons in the size of  $6.0 \times 2.0 \times 0.3$  cm were cut from the N80 steel casing (supplied by ONGC) with a small hole  $\approx 2$  mm diameter at the upper edge of specimen for weight loss studies. For electrochemical studies the size of the electrodes was  $1 \times 1 \times 1$  cm with a 4 cm long tag for electrochemical

contact. N80 steel sample used for the study was analyzed in MET-CHEM Laboratories, Baroda, India and found to have the composition, C(0.31%), S(0.008%), P(0.010%), Si(0.19%), Mn(0.92%), Cr(0.20%) and Fe the rest. The corrosive solution was 15% HCl, obtained by dilution of hydrochloric acid (Emerk, sp gravity  $\approx 1.18$ ) with distilled water. The inhibitor concentration in weight loss and electrochemical study was in the range of 10–150 ppm. The volume of test solution for weight loss and for electrochemical measurement was 300 and 150 ml, respectively. The test coupons were mechanically polished with different grades of emery papers and cleaned with acetone and washed with distilled water and finally dried in dry air before every experiment. After weighing accurately, the specimens were immersed in 300 ml of 15% HCl with and without the addition of different concentrations of inhibitors. After 6 h the coupons were taken out, washed, dried and weighed accurately. The temperature (30–50 °C) experiments were also carried out for a period of 6 h using water circulated Ultra thermostat (model NBE, Germany) with an accuracy of  $\pm 0.5$  °C. Duplicate experiments were performed in each and the mean value of weight loss was reported. The corrosion inhibition ability of an inhibitor is expressed in terms of inhibitor efficiency and is determined by the percentage decrease in corrosion rate after inhibition test.

$$\%IE = \left( \frac{CR^{\circ} - CR}{CR^{\circ}} \right) \times 100 \quad (1)$$

where,  $CR^{\circ}$  = corrosion rate in the absence of inhibitor,  $CR$  = corrosion rate in the presence of inhibitor.

Corrosion rate ( $CR$ ) for the specimen can be calculated in millimeter penetration per years (mmpy) with the help of the following equation:

$$\text{Corrosion rate} = \frac{87.6 \times \Delta W}{DAT} \quad (2)$$

where,  $T$  = exposure time in hours,  $\Delta W$  = weight loss of metal coupons in mg,  $A$  = area of the test coupons in square inches,  $D$  = density of the steel.

The potentiodynamic polarization curves were recorded in the absence and presence of the inhibitors at different concentrations with N80 steel (area  $1 \text{ cm}^2$ ) as working electrode using Potentiostat (VoltaLab 10) at 25 °C. Experiments were performed with saturated calomel electrode as reference electrode and platinum as counter electrode. The potentiodynamic polarization study has been carried out at a steady state and at a scan rate of 10 mV/s and potential range from  $-400$  to  $-550$  mV. From the anodic and cathodic polarization curves, Tafel slopes ( $\beta_a$  and  $\beta_c$ ) and corrosion current ( $i_{\text{corr}}$ ) were

obtained. For calculating %IE by electrochemical polarization method we use the following formula:

$$\%IE = \frac{I_0 - I_{inh}}{I_0} \times 100 \quad (3)$$

where,  $I_0$  = corrosion current in the absence of inhibitor,  $I_{inh}$  = corrosion current in the presence of inhibitor.

AC-impedance studies were carried out in a three electrode cell assembly using computer controlled VoltaLab 10 electrochemical analyser, using N80 steel as the working electrode, platinum as counter electrode and saturated calomel as reference electrode. The data were analyzed using Voltmaster 4.0 software. The electrochemical impedance spectra (EIS) were acquired in the frequency range 10 kHz–1 mHz at the rest potential by applying 10 mV sine wave AC voltage. The charge transfer resistance ( $R_{ct}$ ) and double layer capacitance ( $C_{dl}$ ) were determined from Nyquist plots. The inhibition efficiencies were calculated from charge transfer resistance values by using the following formula:

$$\%IE = \frac{R_{ct(Inh)} - R_{ct}}{R_{ct(Inh)}} \times 100 \quad (4)$$

where,  $R_{ct}$  = charge transfer resistance in the absence of inhibitor,  $R_{ct(Inh)}$  = charge transfer resistance in the presence of inhibitor.

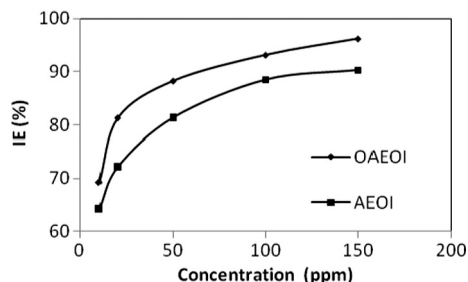
Fourier transform infrared spectroscopic analysis was performed by Perkin Elmer FTIR, (model spectrum – 2000) on the corrosion product removed from metal panels after the immersion tests in the presence of the inhibitors. Morphology of the metal surface was studied with the help of scanning electron microscope model SEM Jeol JSM-5800. SEM micrographs were obtained for polished metal surface, metal surface exposed to 15% HCl solution for 6 h with and without inhibitor/inhibitor mixtures.

### 2.1. Synthesis of inhibitors

The imidazoline derivatives AEOI and OAEOI were synthesized by the reaction of oleic acid with diethylenetriamine in

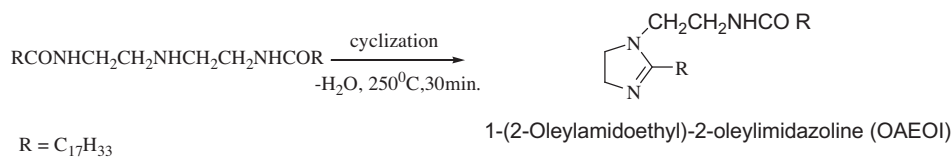
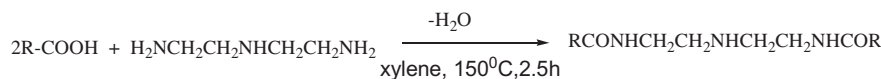
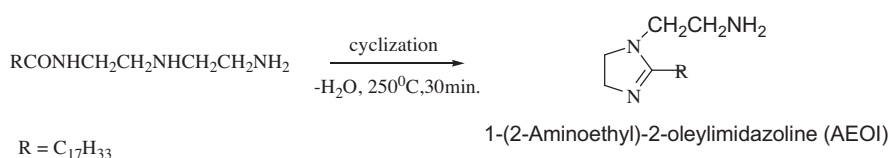
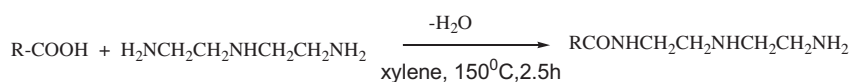
**Table 1** Effect of inhibitors concentration on corrosion of N80 steel at 25 °C.

Conc. (ppm)	OAEOI		AEOI	
	CR (mmpy)	%IE	CR (mmpy)	%IE
0	9.54	–	9.54	–
10	2.93	69.25	3.41	64.25
20	1.97	81.32	2.66	72.16
50	1.02	88.26	1.78	81.36
100	0.46	93.16	1.1	88.45
150	0.26	96.23	0.93	90.26



**Figure 1** Inhibition efficiency (%IE) vs. concentration (ppm) of OAEOI and AEOI at 25 °C.

xylene as the solvent in 1:1 and 1:2 M ratio, respectively (Wang et al., 2003). The synthesis process was carried out in a three-necked flask with thermometer, stirrer and water splitter. The reactant was refluxed at 140–150 °C until no more water came over from the water splitter. The water splitter was removed, the pressure of the reaction system was adjusted to 14.12 kPa, and the reaction temperature was raised to 250 °C for another 30 min. The desired product was obtained. The purity of the product was checked by TLC. The yield was found to be 82% and 86%, respectively.



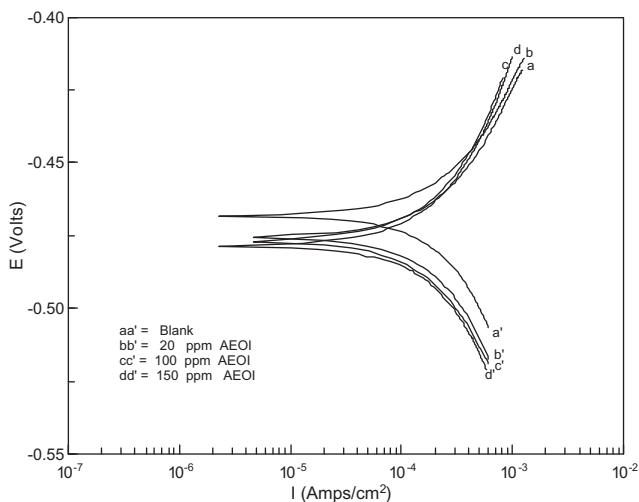


**Figure 2** Polarization curves for N80 steel in 15% HCl containing various concentrations of AEOI at 25 °C.

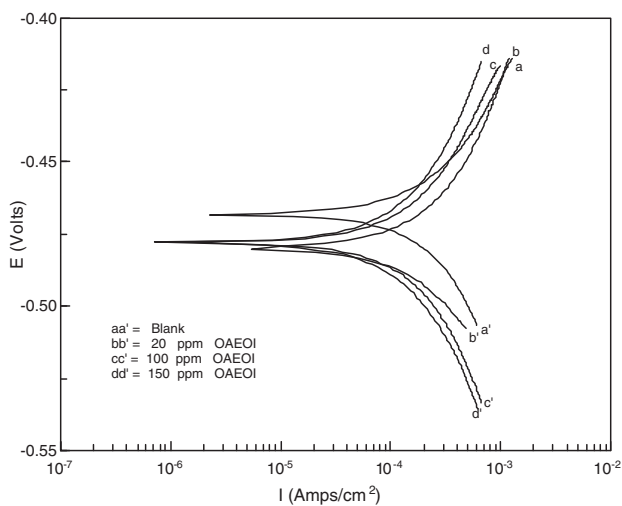


**Figure 3** Polarization curves for N80 steel in 15% HCl containing various concentrations of OAEIOI at 25 °C.

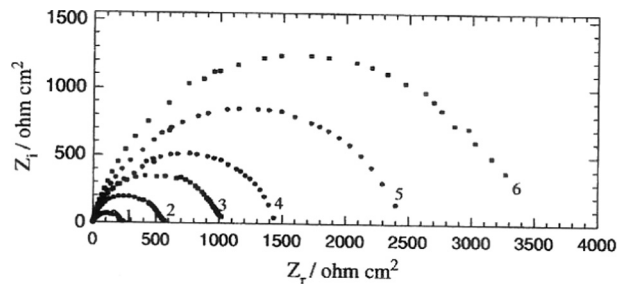


**Figure 4** Nyquist plot for N80 steel in 15% HCl acid containing various concentrations of OAEIOI (1) 0.0 ppm (2) 10 ppm (3) 20 ppm (4) 50 ppm (5) 100 ppm (6) 150 ppm at 25 °C.

**Table 3** Equivalent circuit parameters and inhibition efficiency for N80 steel in 15% HCl acid in the presence of OAEIOI at 25 °C.

Conc. (ppm)	$R_{ct}$ ( $\Omega$ cm <sup>2</sup> )	$C_{dl}$ ( $\mu$ F cm <sup>-2</sup> )	%IE
0	182	34.35	–
10	587	26.54	68.99
20	1015	23.65	82.07
50	1460	21.26	87.53
100	2450	18.38	92.57
150	3466	15.76	94.75

**3. Results and discussion**

*3.1. Weight loss tests*

The percentage inhibition efficiencies (%IE) in the presence of 10, 20, 50, 100 and 150 ppm of AEOI and OAEIOI have been evaluated by weight loss technique after 6 h of immersion and at 25 °C. The corrosion rate (CR) and inhibition efficiency obtained by weight loss data are shown in Table 1. It is evident from these values that both the inhibitors are significantly effective even at low concentrations, like 10 ppm and there is a linear increase in %IE in the whole range of concentrations studied. The variation in inhibition efficiency with concentration is shown in Fig. 1. It is evident from Fig. 1 that inhibition efficiencies (IE) of both the inhibitors increase with increase in concentration and becomes more or less constant at 150 ppm.

**Table 2** Potentiodynamic polarization parameters of the corrosion of N80 steel in 15% HCl in the absence and presence of different concentrations of OAEIOI and AEOI at 25 °C.

Inhibitors	Conc. of Inhibitors (ppm)	Tafel slope		$I_{corr}$ ( $\mu$ A cm <sup>-2</sup> )	$E_{corr}$ (mV)	%IE	%IE from wt. loss
		Anodic $\beta_a$	Cathodic $\beta_c$				
Blank	0	109	153	471.4	–468	–	–
OAEIOI	20	135	181	84.9	–480	82.45	81.32
	100	142	186	37.7	–477	92.26	93.16
	150	148	198	23.6	–477	95.01	96.23
AEOI	20	132	178	136.7	–474	71.33	72.16
	100	140	182	108.4	–475	87.16	88.45
	150	146	191	42.4	–478	91.16	90.26

**Table 4** Immersion test result of N80 steel in 15% HCl in the presence of 150 ppm concentration of inhibitors at different temperature (303–323 K).

Inhibitor	Temp (K)	%IE	CR (mmpy)	$\Delta H$ (kJ/mol)	$E_a$ (kJ/mol)	$\Delta G_{ads}$ (kJ/mol)	$\Delta S$ (J/mol)
Blank	298	–	9.54	–35.64	38.9	–	–
	303		12.09				
	313		19.27				
	323		30.42				
OAEIOI	298	96.23	0.26	–89.65	72.63	–68.75	–21.17
	303	89.45	1.28				
	313	83.16	3.25				
	323	76.43	7.17				
AEIOI	298	90.26	0.93	–94.40	66.18	–52.12	–31.20
	303	85.16	1.79				
	313	78.14	4.21				
	323	70.37	9.01				

### 3.2. Electrochemical polarization studies

Electrochemical polarization behavior in the presence of 20, 100 and 150 ppm of AEIOI and OAEIOI for N80 steel in 15% HCl at 25 °C is shown in Figs. 2 and 3 and various parameters obtained are given in Table 2. The curves in Figs. 2 and 3, illustrate that the nature of the curve remains almost same even after the addition of the inhibitors and also on increasing the concentration of the inhibitors indicating that the inhibitor molecules retard the corrosion process without changing the mechanism of corrosion process in the medium of investigation (Rastogi et al., 2003). The anodic and cathodic polarization curves shifted toward lower current density in the presence of both the inhibitors indicating the mixed nature of the inhibitors. The increase in the cathodic and anodic Tafel slopes ( $\beta_c$  and  $\beta_a$ ) is related to the decrease in both the cathodic and anodic currents. The minor shift in the value of corrosion potential ( $E_{corr.}$ ) in the presence of both the inhibitors also support the mixed nature of the inhibitors (Badr, 2009).

### 3.3. Electrochemical impedance spectroscopy (EIS)

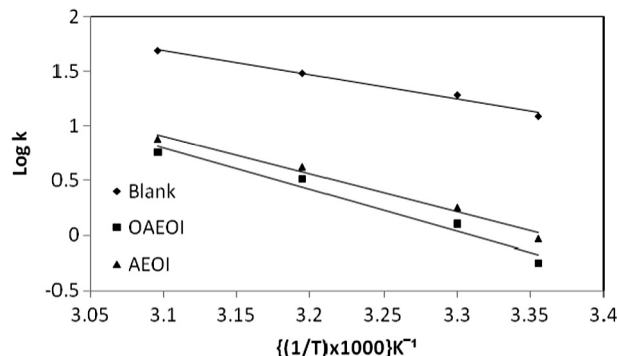
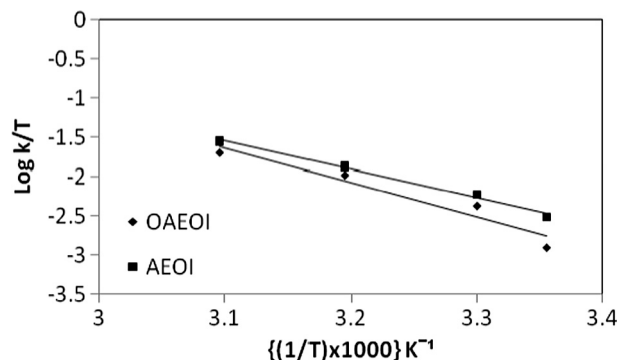
The impedance data of N80 steel, recorded in the presence of 10, 20, 50, 100 and 150 ppm of the inhibitor OAEIOI in 15% HCl solution at 25 °C as Nyquist plots are shown in Fig. 4. The calculated equivalent circuit parameters for N80 steel in 15% HCl solution at 25 °C in the presence of 10, 20, 50, 100 and 150 ppm of the inhibitor is presented in Table 3. From the data in Table 3, it is clear that the value of  $R_{ct}$  increases on increasing the concentration of the inhibitor, indicating that the corrosion rate decreases in the presence of the inhibitor. It is also clear that the value of  $C_{dl}$  decreases on the addition of inhibitors, indicating a decrease in the local dielectric constant and/or an increase in the thickness of the electrical double layer, suggesting the inhibitor molecules function by the formation of the protective layer at the metal surface (Ahamad et al., 2010).

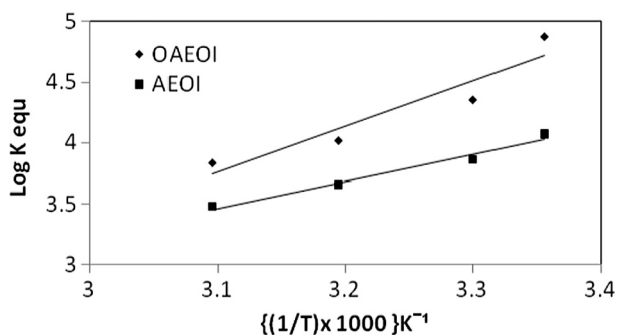
In order to confirm the potentiodynamic results, the corrosion inhibition efficiencies (IE) in the presence of 10, 20, 50, 100 and 150 ppm concentrations of the inhibitor OAEIOI in 15% HCl acid at 25 °C were also calculated from the corresponding electrochemical impedance data and is given in

Table 3. The corrosion inhibition efficiencies calculated from impedance data are in good agreement with those obtained from electrochemical polarization data and weight loss measurement.

### 3.4. Effect of temperature and thermodynamic parameters of inhibitor adsorption

Experiments were carried out at different temperature (298–323 K) in the presence of 150 ppm of inhibitors. It has been found that the corrosion rate increases with the increase in

**Figure 5** Arrhenius plot for AEIOI and OAEIOI.**Figure 6** Transition state plot for AEIOI and OAEIOI.



**Figure 7** Variation of  $\log K_{\text{equ}}$  with  $1/T$  for N80 steel in 15% HCl in presence of OAEOI and AEOI.

temperature for both the inhibitors (Table 4). The corrosion rate of N80 steel in the absence of inhibitors increased steeply from 303 to 323 K whereas, in the presence of inhibitors the corrosion rate increased slowly. The inhibition efficiency was found to decrease with temperature. The results show that the inhibition efficiency offered by AEOI and OAEOI was 70.37% and 76.43%, respectively at 323 K. The corrosion parameter in the absence and presence of inhibitors in the temperature range 298–323 K has been summarized in Table 4.

The apparent activation energy ( $E_a$ ) for dissolution of N80 steel in 15% HCl was calculated from the slope of plots by using Arrhenius equation:

$$\log k = -E_a/2.303 RT + \log A \quad (5)$$

where  $k$  is rate of corrosion,  $E_a$  is the apparent activation energy,  $R$  is the universal gas constant,  $T$  is absolute temperature and  $A$  is the Arrhenius pre-exponential factor. By plotting  $\log k$  against  $1/T$  the values of activation energy ( $E_a$ ) has been calculated ( $E_a = -(\text{slope}) \times 2.303 \times R$ ) (Fig. 5). Activation energy for the reaction of N80 steel in 15% HCl increases in the presence of inhibitors (Table 4). The increase in activation energy  $E_a$  indicates the retardation in corrosion rate which could have occurred because of adsorption of the inhibitors at the surface of the metal (Popova et al., 2003).

The values of change of entropy ( $\Delta S$ ) and change of enthalpy ( $\Delta H$ ) can be calculated by using the formula:

$$k = (RT/Nh) \exp(\Delta S/R) \exp(\Delta H/RT) \quad (6)$$

where  $k$  is rate of corrosion,  $h$  is Planks constant,  $N$  is Avogadro number,  $\Delta S$  is the entropy of activation, and  $\Delta H$  is the enthalpy of activation. A plot of  $\log(k/T)$  vs.  $1/T$  (Fig. 6) should give a straight line, with a slope of  $(-\Delta H/2.303R)$  and an intercept of  $[\log(R/Nh) + \Delta S/2.303R]$ , from which the values of  $\Delta S$  and  $\Delta H$  can be calculated (Table 4).

The negative value of  $\Delta S$  (Table 4) for both the inhibitors indicates that activated complex in the rate determining step represents an association rather than a dissociation step, meaning that a decrease in disorder takes place during the course of transition from reactant to the activated complex (Saliyan and Adhikari, 2007). The negative sign of  $\Delta H$  indicates that the adsorption of inhibitor molecules is an exothermic process. Generally, an exothermic process signifies either physisorption or chemisorption or a combination of both. Typically, the enthalpy of physisorption process is lower than that of 40.00 kJ/mol while the enthalpy of chemisorptions process approaches 100 kJ/mol (Kosari et al., 2011). In the present study the

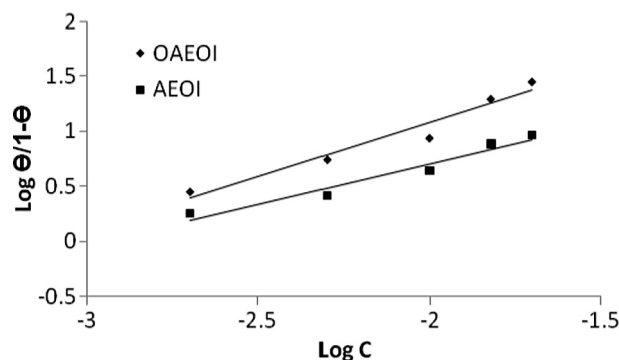


**Figure 8** Langmuir plots for AEOI and OAEOI.

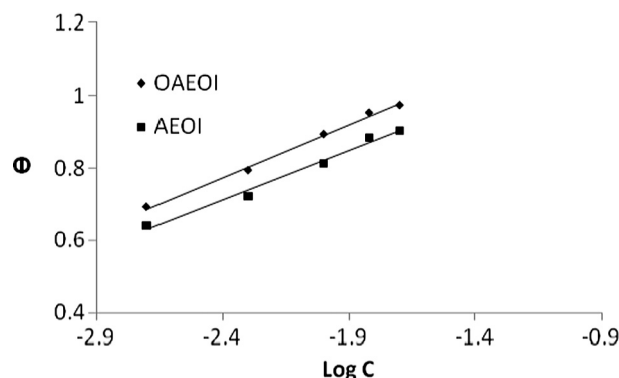


**Figure 9** Temkin plots for AEOI and OAEOI.

absolute value of the heat of adsorption  $\Delta H^\circ$  for AEOI and OAEOI was found  $-94.40$  and  $-89.65$  kJ/mol (Table 4), indicating the chemisorptions of the inhibitors at the surface of N80 steel. The average values for free energy of adsorption ( $\Delta G_{\text{ads}}$ ), were calculated using the following equation:

$$K = \frac{1}{55.5} \exp\left(\frac{-\Delta G_{\text{ads}}}{RT}\right) \quad (7)$$

where  $\theta$  is degree of coverage on metal surface,  $C$  is concentration of inhibitors in  $\text{mol l}^{-1}$ ,  $R$  is molar gas constant in  $\text{J K}^{-1} \text{mol}^{-1}$  and  $T$  is temperature. The value of 55.5 in the above equation is the concentration of water in the solution in mol/liter. The equilibrium constant ( $K$ ) has been replaced by the equation  $\left[K = \frac{\theta}{(1-\theta) \times C}\right]$ . By plotting  $\log k$  against  $1/T$  the value of  $\Delta G_{\text{ads}}$  can be calculated ( $\Delta G_{\text{ads}} = -2.303 \times R \times \text{Slope}$ ) from the slope of the straight line obtained (Fig. 7). The standard free energy of adsorption ( $\Delta G_{\text{ads}}$ ) for AEOI and OAEOI was found to be  $-52.12$  and  $-68.75$  kJ/mol (Table 4), respectively, indicating that the inhibitors were adsorbed on the metal surface by chemisorption (Tao et al., 2009). The negative values indicate the spontaneity of the adsorption process and stability of the adsorbed layer on N80 steel surface.

### 3.5. Adsorption isotherms

The mechanism of corrosion inhibition may be explained on the basis of adsorption behavior. The most frequently used

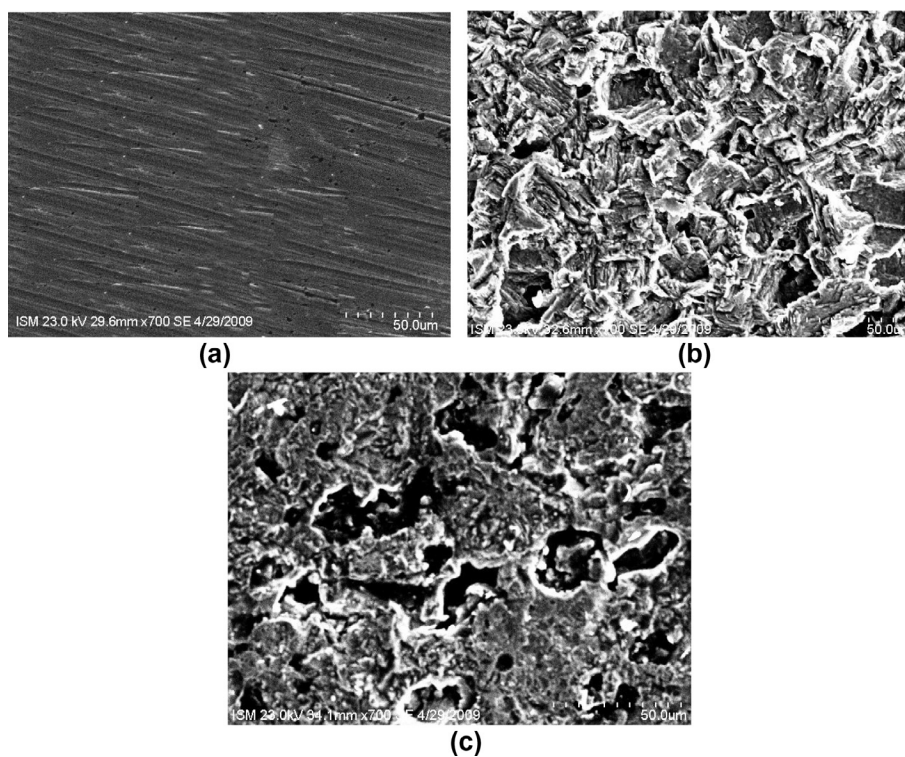


**Figure 10** SEM of (a) polished sample (b) sample in presence of 15% hydrochloric acid (c) sample in presence of 150 ppm of OAEI.

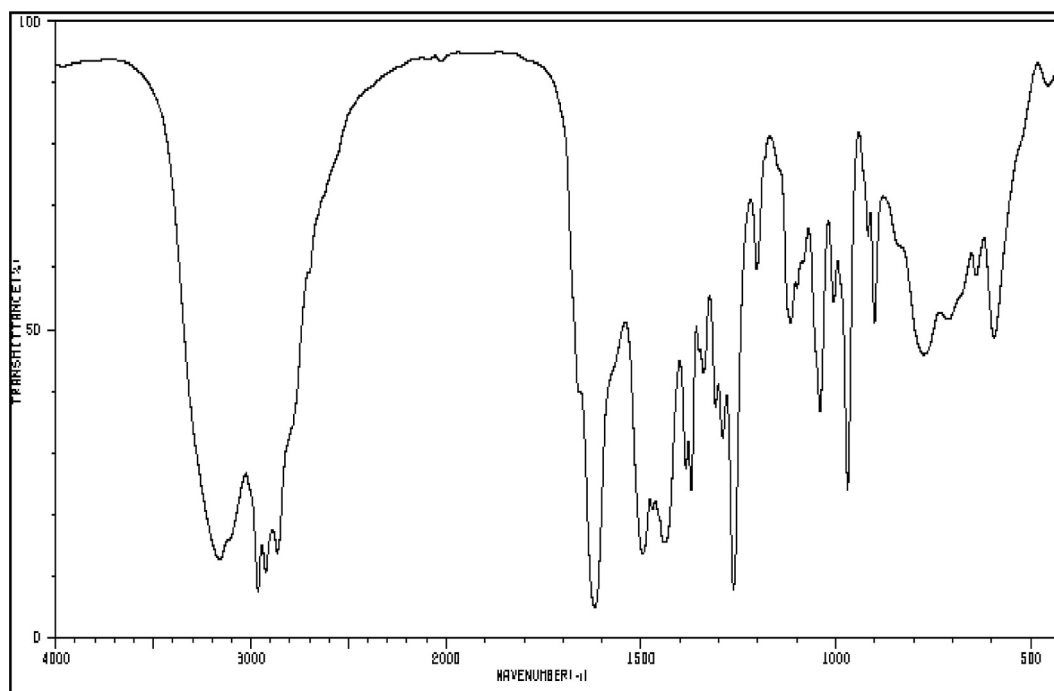


**Figure 11** FTIR spectrum of surface product formed on the metal after the corrosion test in presence of inhibitor AEOI.

adsorption isotherms are Langmuir, Temkin, and Frumkin. The degree of surface coverage ( $\theta$ ) for different concentrations of inhibitor in 15% hydrochloric acid has been evaluated by

weight loss value. The data were tested graphically by fitting to various isotherms. A straight line is obtained on plotting  $\log(\theta/1-\theta)$  and  $\theta$  against  $\log C$  (Figs. 8 and 9) suggesting that

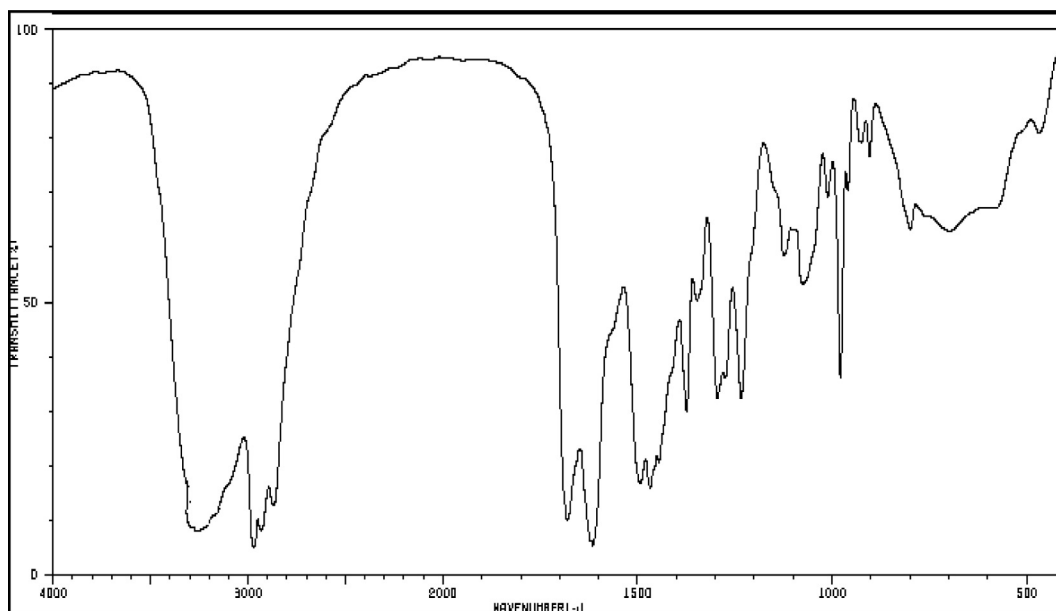


**Figure 12** FTIR spectrum of surface product formed on the metal after the corrosion test in the presence of inhibitor OAEIO.

adsorption of the compound on the surface of N80 steel follows Langmuir as well as Temkin adsorption isotherm (Singh et al., 2003).

### 3.6. SEM study

Fig. 10 (a, b, c, d) shows the microphotographs for N80 steel in 15% hydrochloric acid in the absence and presence of 150 ppm of OAEIO at 200 $\times$  magnification. On comparing these micrographs, it appears that in the presence of inhibitors, the surface of the test material has improved remarkably with respect to its smoothness. The smoothening of the surface would have been caused by the adsorption of inhibitor molecules on it and thus, the surface is fully covered.

### 3.7. FTIR spectroscopic analysis of corrosion product

The products formed on the metal surface after the corrosion test in acid in the presence of the AEOI and OAEIO were analyzed using the FTIR spectrophotometer (Figs. 11 and 12). A band at 3210 and 3250  $\text{cm}^{-1}$  (Finar, 1998) was observed for AEOI and OAEIO, respectively, which may indicate N–H stretching for amino group present in AEOI and OAEIO. A peak observed at 2980 and 2990  $\text{cm}^{-1}$  in the spectrum of AEOI and OAEIO, respectively, indicates C–H stretching of methyl group. A peak at 1620 and 1610  $\text{cm}^{-1}$  in the spectrum of AEOI and OAEIO, respectively, indicated N=C–N stretching of imidazoline ring. A peak at 1690  $\text{cm}^{-1}$  in the spectrum is attributed to C=O stretching of carbonyl group. The presence of all the groups present in pure AEOI and OAEIO in the spectrum of the surface product indicate the adsorption of inhibitors AEOI and OAEIO at the surface of N80 steel.

## 4. Discussion

The protective action of the inhibitors AEOI and OAEIO were considered in the context of their adsorption on the metal

surface. In acid solution, the inhibitors can exist as protonated species which may be adsorbed through electrostatic interaction between the positively charged inhibitor molecules and the negatively charged metal surface. Adsorption of the unprotonated inhibitors AEOI and OAEIO on the metal may occur by the interaction between the vacant d-orbital of iron atom at the surface and the lone pair electron of nitrogen atom present in the inhibitors. The mechanism of inhibition of corrosion is believed to be through the formation of a protective film on the metal surface. Further, when  $\log(\theta/1-\theta)$  and  $\theta$  are plotted against  $\log C$ , straight lines are obtained for both the inhibitors (Figs. 8 and 9) suggesting inhibitors adsorption following Langmuir isotherm and Tempkin isotherm. The inhibition efficiency of OAEIO is higher than that of AEOI due to its larger size and the presence of more number of active atoms. The adsorption is occurring through nitrogen of amino group and nitrogen and delocalized  $\pi$ -electrons of the imidazoline ring. The presence of  $\pi$ -electrons of the imidazoline ring and large hydrophobic hydrocarbon chain facilitates the adsorption process at the surface of the metal. The lowering of inhibition efficiency with temperature may be due to higher desorption rate at higher temperature. The increase in activation energy in the presence of inhibitors is due to the formation of a barrier at the surface of the steel which prevents the dissolution of the metal. The negative value of  $G_{\text{ads}}$  and  $\Delta H$  indicate that the adsorption is spontaneous and exothermic process, respectively.

## 5. Conclusions

Both the inhibitors AEOI and OAEIO act as efficient corrosion inhibitors for N80 steel in 15% HCl solution. OAEIO shows appreciably higher efficiency than the AEOI due to the presence of more number of active centers and larger size as compared to the inhibitor AEOI. Both the inhibitors act as mixed inhibitors. It is suggested from the results obtained from SEM and Langmuir adsorption isotherm that the

mechanism of corrosion inhibition is occurring through adsorption process. EIS measurements show that charge transfer resistance ( $R_{ct}$ ) increases and double layer capacitance ( $C_{dl}$ ) decreases in the presence of inhibitors indicating the adsorption of the inhibitors at the surface of N80 steel.

## References

- Ahamad, Istiaque, Prasad, Rajendra, Quraisi, M.A., 2010. Adsorption and inhibitive properties of some new mannich bases of isatine derivatives on corrosion of mild steel in acid media. *Corros. Sci.* 52, 1472–1481.
- Allen, T.O., Roberts, A.P., 1982. In: *Production Operations*, vol. 2. Oil & Gas Consultants International, Tulsa, OK, p. 89.
- Ashassi-Sorkhabi, H., Majidi, M.R., Seyyedi, K., 2004. Investigation of inhibition effect of some amino acids against steel corrosion in HCl solution. *Appl. Surf. Sci.* 225, 176–185.
- Badr, G.E., 2009. The role of some thiosemicarbazide derivatives as corrosion inhibitors for C-steel in acid media. *Corros. Sci.* 51, 2529–2536.
- Emranuzaman, Kumar, T., Vishwanatham, S., Udaybhanu, G., 2004. Synergistic effect of formaldehyde and alcoholic extract of plants leaves for protection of N80 steel in 15% HCl. *Corros. Eng., Sci. Technol.* 39, 327–332.
- Finar, I.L., 1998. In: *Organic Chemistry Fundamental principle*, vol. 1. Addison Wesley, London, p. 655.
- Ghareba, Sad, Omanic, Saha, 2010. Interaction of 12-aminododecanoic acid with a carbon steel surface: Towards the development of green corrosion inhibitors. *Corros. Sci.* 52, 2104–2113.
- Hluchan, V., Wheeler, B.L., Hackerman, N., 1998. Amino acids as corrosion inhibitors in hydrochloric acid solutions. *Mater. Corros.* 39, 512–517.
- Khaled, K.F., 2008. New synthesized guanidine derivatives as a green corrosion inhibitor for mild steel in acid solution. *Int. J. Electrochem. Sci.* 3, 462–475.
- Kosari, A., Momeni, M., Parvizi, R., Zakeri, M., Moayed, M.H., Davoodi, A., Eshghi, H., 2011. Theoretical and electrochemical assessment of inhibitive behavior of some thiophenol derivatives on mild steel in HCl. *Corros. Sci.* 53, 3058–3067.
- Neemla, K.D., Jayaraman, A., Saxena, R.C., Agrawal, A.K., Krishna, R., 1989. Corrosion inhibitor studies on oil well tubular steels in hydrochloric acid. *Bull. Electrochem.* 5, 250–253.
- Popova, A., Sokolova, E., Raicheva, S., Chritov, M., 2003. AC and DC study of the temperature effect on mild steel corrosion in acid media in presence of benzimidazole derivatives. *Corros. Sci.* 45, 33–41.
- Quraisi, M.A., Sardar, N., Ali, H., 2002. A study of some new acidizing inhibitors on corrosion of N80 alloy in 15% boiling hydrochloric acid. *Corrosion* 58, 317–321.
- Rastogi, R.B., Singh, M.M., Yadav, M., 2003. Substituted thiobiurets and their molybdenum and tungsten complexes as corrosion inhibitors for mild steel in 1.0 N sulphuric acid. *J. Eng. Mater. Sci.* 10, 155–160.
- Singh, M.M., Rastogi, R.B., Yadav, M., 2003. Thiosemicarbazide, phenyl isothiocyanate and their condensation product as inhibitors for corrosion of copper in aqueous chloride solution. *Mater. Chem. Phys.* 80, 283–293.
- Tao, Zhihua, Zhang, Shengtao, Li, Weihua, Hou, Baorong, 2009. Corrosion inhibition of mild steel in acidic solution by some oxotriazole derivatives. *Corros. Sci.* 52, 2588–2599.
- Ramesh Saliyan, V., Vasudeva Adhikari, Airody, 2007. Inhibition of corrosion of mild steel in acid media by N'-benzylidene-3-(quinolin-4-ylthio)propanohydrazide. *Bull. Mater. Sci.* 31 (4), 699–711.
- Vishwanatham, S., Sinha, P.K., 2009. Corrosion protection of N80 steel in HCl by condensation products of aniline and phenol. *Anti-Corrosion Methods Mater.* 56 (3), 139–144.
- Wang, Shi-Fa, Furuno, Takeshi, Cheng, Zhi, 2003. Synthesis of 1-hydroxyethyl-2-alkyl-2-imidazoline and its derivative sulfonate amphoteric surfactant from tall oil fatty acid. *J. Wood Sci.* 49, 371–376.
- Yadav, M., Sharma, U., 2011. Eco-friendly corrosion inhibitors for N80 steel in hydrochloric acid. *J. Mater. Environ. Sci.* 2 (4), 407–414.